



# Molecular and Optical Properties of Tree-Derived Dissolved Organic Matter in Throughfall and Stemflow from Live Oaks and Eastern Red Cedar

Aron Stubbins<sup>1\*</sup>, Leticia M. Silva<sup>1</sup>, Thorsten Dittmar<sup>2</sup> and John T. Van Stan<sup>3</sup>

<sup>1</sup> Department of Marine Sciences, Skidaway Institute of Oceanography, University of Georgia, Savannah, GA, USA,

<sup>2</sup> Research Group for Marine Geochemistry, Institute for Chemistry and Biology of the Marine Environment, University of Oldenburg, Oldenburg, Germany, <sup>3</sup> Department of Geology and Geography, Georgia Southern University, Statesboro, GA, USA

## OPEN ACCESS

### Edited by:

Richard G. Keil,  
University of Washington, USA

### Reviewed by:

David Christopher Podgorski,  
Florida State University, USA  
Christian Schlosser,  
GEOMAR Kiel, Germany

### \*Correspondence:

Aron Stubbins  
aron.stubbins@skio.uga.edu

### Specialty section:

This article was submitted to  
Marine Biogeochemistry,  
a section of the journal  
Frontiers in Earth Science

**Received:** 28 November 2016

**Accepted:** 20 February 2017

**Published:** 28 March 2017

### Citation:

Stubbins A, Silva LM, Dittmar T and  
Van Stan JT (2017) Molecular and  
Optical Properties of Tree-Derived  
Dissolved Organic Matter in  
Throughfall and Stemflow from Live  
Oaks and Eastern Red Cedar.  
*Front. Earth Sci.* 5:22.  
doi: 10.3389/feart.2017.00022

Studies of dissolved organic matter (DOM) transport through terrestrial aquatic systems usually start at the stream. However, the interception of rainwater by vegetation marks the beginning of the terrestrial hydrological cycle making trees the headwaters of aquatic carbon cycling. Rainwater interacts with trees picking up tree-DOM, which is then exported from the tree in stemflow and throughfall. Stemflow denotes water flowing down the tree trunk, while throughfall is the water that drips through the leaves of the canopy. We report the concentrations, optical properties (light absorbance) and molecular signatures (ultrahigh resolution mass spectrometry) of tree-DOM in throughfall and stemflow from two tree species (live oak and eastern red cedar) with varying epiphyte cover on Skidaway Island, Savannah, Georgia, USA. Both stemflow and throughfall were enriched in DOM compared to rainwater, indicating trees were a significant source of DOM. The optical and molecular properties of tree-DOM were broadly consistent with those of DOM in other aquatic ecosystems. Stemflow was enriched in highly colored DOM compared to throughfall. Elemental formulas identified clustered the samples into three groups: oak stemflow, oak throughfall and cedar. The molecular properties of each cluster are consistent with an autochthonous aromatic-rich source associated with the trees, their epiphytes and the microhabitats they support. Elemental formulas enriched in oak stemflow were more diverse, enriched in aromatic formulas, and of higher molecular mass than for other tree-DOM classes, suggesting greater contributions from fresh and partially modified plant-derived organics. Oak throughfall was enriched in lower molecular weight, aliphatic and sugar formulas, suggesting greater contributions from foliar surfaces. While the optical properties and the majority of the elemental formulas within tree-DOM were consistent with vascular plant-derived organics, condensed aromatic formulas were also identified. As condensed aromatics are generally interpreted

as deriving from partially combusted organics, some of the tree-DOM may have derived from the atmospheric deposition of thermogenic and other windblown organics. These initial findings should prove useful as future studies seek to track tree-DOM across the aquatic gradient from canopy roof, through soils and into fluvial networks.

**Keywords:** Tree-DOM, dissolved organic matter (DOM), carbon, CDOM, deposition, dissolved organic carbon (DOC), stemflow, throughfall

## INTRODUCTION

In forested catchments, trees represent the first interceptors of precipitation and the first potential source of dissolved organic matter (DOM) to the aquatic carbon cycle. The earliest trees appear in the fossil record approximately 385 million years ago (Stein et al., 2007), since when they have fundamentally altered terrestrial (Algeo et al., 2001; Gensel, 2001) and wetland ecosystems (Greb et al., 2006). Forests are estimated to have covered close to 50 million km<sup>2</sup> of the planet 5,000 years ago (FAO, 2016) equivalent to approximately 1/3rd of the earth's land surface. Just as forests transformed the global ecosystem, humans now have a similarly profound influence upon global ecology and biogeochemistry. Deforestation during the Anthropocene (Crutzen, 2002) has seen forest land cover reduced by approximately 50% to 31.7 million km<sup>2</sup> as of 2005 (Hansen et al., 2010) and was continuing at a rate of approximately 1.5 million km<sup>2</sup> year<sup>-1</sup> between 2000 and 2012 (Hansen et al., 2013).

Despite the vast and rapidly changing expanse of land covered and volume of precipitation intercepted by trees, only modest attention has been focused upon the DOM delivered by trees to downstream ecosystems (Kolka et al., 1999; Michalzik et al., 2001; Neff and Asner, 2001; Levia et al., 2011; Inamdar et al., 2012). Once intercepted, rainwater takes one of two hydrological flow paths to the forest floor: throughfall (water that drips from the canopy or falls directly through canopy gaps) and stemflow (water funneled by the canopy to the stem). Both stemflow (5–200 mg-C L<sup>-1</sup>) (Moore, 2003; Tobón et al., 2004; Levia et al., 2011) and throughfall (1–100 mg-C L<sup>-1</sup>) (Michalzik et al., 2001; Neff and Asner, 2001; Le Mellec et al., 2010; Inamdar et al., 2012) are enriched in DOM relative to rainwater (0.3–2 mg-C L<sup>-1</sup>) (Willey et al., 2000).

The fate of exported tree-derived DOM (tree-DOM) will depend upon the chemistry of the tree-DOM, the nature of the receiving ecosystem and hydrological considerations. Significant losses and alteration of tree-DOM occurs as stemflow and throughfall enter soils due to sorption to mineral soils, which preferentially retain hydrophobic DOM fractions (Jardine et al., 1989; Kaiser and Zech, 1998, 2000). The spatially and temporally uneven delivery of biolabile tree-DOM to soil ecosystems during storms may fuel biogeochemical hot spots and hot moments (McClain et al., 2003; Vidon et al., 2010) and microbial utilization of biolabile organics in soils further modifies tree-DOM (Aitkenhead-Peterson et al., 2003). It has also been suggested that sunlight driven photoreactions (Mopper et al., 2015) may act as a sink for tree-DOM (Aitkenhead-Peterson et al., 2003). Photoreactions would be expected to preferentially

remove aromatics, including black carbon (Stubbins et al., 2012b), while preserving and producing high H/C compounds such as aliphatics (Stubbins et al., 2010; Stubbins and Dittmar, 2015).

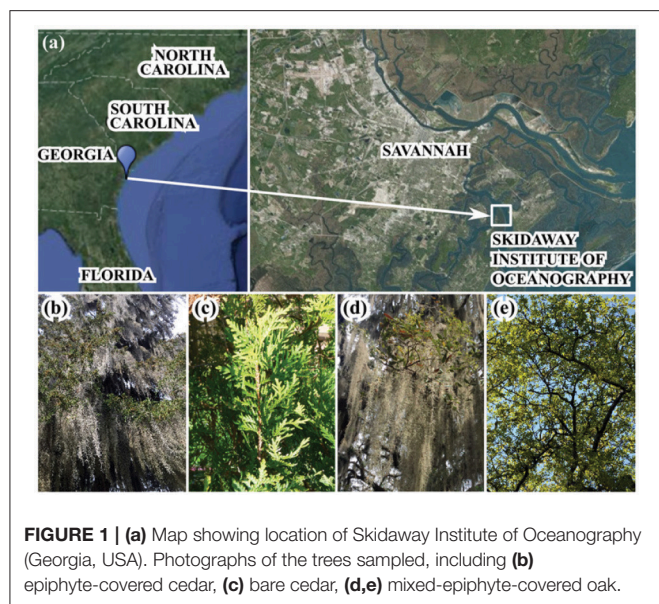
The degree to which tree-DOM is lost and altered by these processes before reaching a downstream aquatic ecosystem also depends upon the flow path traveled down the tree and from there to an inland water body (Inamdar et al., 2012). Direct input of stemflow or throughfall into a stream or lake will presumably result in negligible alteration prior to delivery. High levels of minimally modified tree-DOM may also reach inland waters during periods of heavy rainfall and resultant high flow when residence times within modifying ecosystems (e.g., soils) are reduced or bypassed completely in the case of overland flow. High flow pulses driven by heavy precipitation shunt reactive DOM downstream through river networks and are increasingly recognized as significant components of the fluvial carbon cycle (Raymond et al., 2016). These extreme, short lived pulses can account for the majority of annual river DOC loads being exported in just a few days per year (Raymond and Saiers, 2010). It remains unclear whether tree-DOM is delivered efficiently to fluvial systems during these pulse-shunt events.

To further understand the quality of tree-DOM, we collected stemflow and throughfall samples from broadleaved (oak) and needleleaved (cedar) trees with or without epiphytes during two storm events. The concentrations, optical properties and molecular signatures of the sampled tree-DOM are presented.

## METHODS

### Sample Site

Samples were collected on the Skidaway Institute of Oceanography (SkIO) campus, Georgia, USA (31.9885°N, 81.0212°W) (**Figure 1a**) during two rain events: Storm A on June 27th 2015 and Storm B on 28th June 2015 (**Table 1**). SkIO is in a subtropical climate zone (Köppen *Cfa*), with 30-year mean annual precipitation ranging from 750 to 1,200 mm that occurs as rainfall and mostly during the summer months (GA Office of the State Climatologist). Average daily temperatures in summer range between 30 and 35°C (Georgia Office of the State Climatologist, 2012). The elevation of SkIO ranges from 0 to 10 m above mean sea level. The sampling sites were flat (0–5% slopes) and underlain by Chipley fine sandy soils (<https://websoilsurvey.sc.egov.usda.gov>). Two species of tree were sampled: *Quercus virginiana* Mill. (southern live oak) referred to here as oak for brevity; and, *Juniperus virginiana* L. (eastern red cedar) referred to as cedar. The epiphytes *Tillandsia usneoides* L. (Spanish moss) and *Pleopeltis polypodioides* (resurrection fern) can be found to



cover these trees at high densities on SkIO (Figures 1b–e). A Spanish moss-covered cedar tree (cedar moss, Figure 1b) and an epiphyte-free cedar tree (bare cedar, Figure 1c) were chosen to assess whether the influence of epiphytes were apparent in the concentrations or quality of tree-DOM. Four oak trees were sampled, each with highly variable epiphyte coverage including, both resurrection ferns and Spanish moss (Figures 1d,e), which is typical of live oaks in the maritime southeastern US. Both stemflow and throughfall samples were collected for each tree type.

### Sample Collection and Processing

All plastic and glassware were pre-cleaned by rinsing five times with ultrapure water (MilliQ), soaking in pH 2 ultrapure water (2 ppt 6N hydrochloric acid), re-rinsing five times with ultrapure water, and dried. Once dry, glassware was further baked at 450°C for 8 h. Twenty throughfall samplers (0.18 m<sup>2</sup>, 0.5 m height, high density polyethylene (HDPE) bins) were deployed for each storm, three beneath each of four oaks (TF Oak 1–4), and four beneath the bare (TF Bare Cedar) and four beneath the epiphyte-covered cedars (TF Cedar Moss). An additional four throughfall samplers were placed upon open ground to sample rainwater (Rain). Stemflow samplers, which consisted of collars cut from polyethylene tubing wrapped about the trunk at 1.4 m height and connected to 10 L HDPE carboys, were installed on four oaks (SF Oak 1–4), the bare cedar (SF Bare Cedar) and the epiphyte-covered cedar (SF Cedar Moss). Throughfall and stemflow collectors were deployed approximately 1 h before rainfall commenced and collected within 1 h of rainfall ceasing. All sampling sites are within 10 min walk of Stubbins' laboratory at SkIO. Samples were rapidly returned to the laboratory and 0.2 μm filtered within 4 h of collection. Sample volumes were measured. Throughfall and rainwater volume fluxes (mm) were calculated by dividing the sample volumes by the surface area of the samplers (0.18 m<sup>2</sup>).

### Dissolved Organic Carbon Concentrations

After filtration, aliquots of sample were transferred to pre-combusted 40 mL glass vials, acidified to pH 2 (hydrochloric acid), and analyzed for non-purgable organic carbon using a Shimadzu TOC-VCPH analyzer fitted with a Shimadzu ASI-V autosampler. In addition to potassium hydrogen phthalate standards, aliquots of deep seawater reference material, Batch 10, Lot# 05-10, from the Consensus Reference Material Project (CRM) were analyzed to check the precision and accuracy of the DOC analyses. Analyses of the CRM deviated by <5% from the reported value for these standards (41–44 μM-DOC). Routine minimum detection limits in the investigator's laboratory using the above configuration are 2.8 ± 0.3 μM-C and standard errors are typically 1.7 ± 0.5% of the DOC concentration (Stubbins and Dittmar, 2012).

### Colored Dissolved Organic Matter

Filtered sample (non-acidified) was placed in a 1 cm quartz absorbance cell situated in the light path of an Agilent 8453 ultraviolet-visible spectrophotometer and CDOM absorbance spectra were recorded from 190 to 800 nm. Ultrapure water provided a blank. Blank corrected absorbance spectra were corrected for offsets due to scattering and instrument drift by subtraction of the average absorbance between 700 and 800 nm (Stubbins et al., 2011). Data output from the spectrophotometer were in the form of dimensionless absorbance (i.e., optical density, OD) and were subsequently converted to the Napierian absorption coefficient,  $a$  (m<sup>-1</sup>) (Hu et al., 2002). If sample absorbance (OD) exceeded 2 at 250 nm, samples were diluted 10-fold with ultrapure water and reanalyzed. Specific UV absorbance at 254 nm (SUVA<sub>254</sub>; L mg-C<sup>-1</sup> m<sup>-1</sup>), an indicator of DOM aromaticity defined as the Decadic absorption coefficient at 254 nm (m<sup>-1</sup>) normalized to DOC (mg-C L<sup>-1</sup>) (Weishaar et al., 2003) was calculated along with spectral slope over the range 275–295 nm ( $S_{275-295}$ ) (Helms et al., 2008). Spectral slope values are reported as positive values.

### Fourier Transform Ion Cyclotron Resonance Mass Spectrometry

In the current study, whole water samples were analyzed without extraction or purification to provide the broadest analytical window prior to mass spectral analysis. Each stemflow sample (SF Oak 1–4; SF Cedar Moss; SF Bare Cedar) was analyzed. For throughfall samples, carbon-weighted composite samples were generated for each rainfall and throughfall sample by combining carbon-dependent volumes of sample (i.e., all four aliquots were combined for each of the rain samples and each cedar sampled for throughfall; three aliquots were combined for each of the four oak trees sampled for throughfall; the volume that each aliquot contributed to a composite sample was adjusted in order that the final composite sample contained an equal fraction of carbon from each aliquot). To generate consistent FT-ICR mass spectra all samples were analyzed under the same conditions, including DOC concentration. Therefore, all tree-DOM samples were diluted to the identical DOC concentration with ultrapure water (10 mg-C L<sup>-1</sup>) and then further diluted 1:1 with methanol. However, as rainwater DOC (1–2 mg-C

**TABLE 1 | Sample numbers, volumes, hydrological fluxes (calculated based upon the 0.18 m<sup>2</sup> surface area of rain and throughfall collectors), dissolved organic carbon concentrations (DOC), colored dissolved organic matter Napierian absorption coefficients at 300 nm (CDOM  $a_{300}$ ), CDOM spectral slope values for the range 275–295 nm ( $S_{275-295}$ ), and specific ultraviolet absorbance at 254 nm (SUVA<sub>254</sub>) for rainwater and each of the stemflow (SF) and throughfall (TF) sample types collected during two storms.**

Event	Sample name	N	Volume (mL)	Flux (mm)	DOC (mg-C L <sup>-1</sup> )	CDOM $a_{300}$ (m <sup>-1</sup> )	$S_{275-295}$ (nm <sup>-1</sup> )	SUVA <sub>254</sub> (L mg-C <sup>-1</sup> m <sup>-1</sup> )
Storm A 27/06/15	Rain	4	2778 ± 125	15 ± 1	2.3 ± 0.1	1.9 ± 0.9	0.0208 ± 0.0037	0.8 ± 0.2
	SF Oak	4	246 ± 140	N/A	46 ± 9	180 ± 83	0.0146 ± 0.0002	3.0 ± 0.9
	TF Oak	12	2172 ± 439	12 ± 2	15 ± 8	43 ± 22	0.0158 ± 0.0008	2.2 ± 0.3
	SF Cedar Moss	1	>10 L	N/A	52	321	0.0154	5.1
	TF Cedar Moss	4	1855 ± 355	10 ± 2	52 ± 9	153 ± 28	0.0165 ± 0.0001	2.4 ± 0.1
	SF Bare Cedar	1	>10 L	N/A	30	159	0.0145	4.1
	TF Bare Cedar	4	2996 ± 197	16.6 ± 1.1	13 ± 1	40 ± 4	0.016 ± 0.0002	2.5 ± 0.1
Storm B 28/06/15	Rain	4	3600 ± 91	20.0 ± 0.5	1.2 ± 0.1	0.7 ± 0.7	0.0457 ± 0.0237	0.8 ± 0.4
	SF Oak	4	1140 ± 674	N/A	78 ± 17	418 ± 99	0.0144 ± 0.0002	4.1 ± 0.1
	TF Oak	12	3488 ± 610	19.4 ± 3.4	10 ± 7	31 ± 19	0.0158 ± 0.0009	2.6 ± 0.4
	SF Cedar Moss	1	9583	N/A	71	378	0.0145	4.0
	TF Cedar Moss	4	2945 ± 200	16.4 ± 1.1	36 ± 9	113 ± 24	0.016 ± 0.0002	2.5 ± 0.2
	SF Bare Cedar	1	>10 L	N/A	25	129	0.0155	4.0
	TF Bare Cedar	4	3358 ± 294	18.7 ± 1.6	13 ± 2	48 ± 13	0.0157 ± 0.0006	2.9 ± 0.3

Values present are means ± one standard deviation.

L<sup>-1</sup>; **Table 1**) was significantly lower than for tree-DOM and reducing all sample DOC concentrations to <1 mg-C L<sup>-1</sup> would have impaired FT-ICR MS performance, rainwater samples were diluted 1:1 with methanol and run at their resulting DOC concentrations (Storm A: 1.1 mg-C L<sup>-1</sup>; Storm B: 0.6 mg-C L<sup>-1</sup>). As this impaired the quality of the rainwater FT-ICR MS data, this data is only used to contrast with the tree-DOM data in a cluster analysis and the molecular quality of rainwater DOM is not presented. In order to compare rainwater DOM to tree-DOM directly, the study design would have needed to include a DOM isolation and concentration step in order to allow all samples, rainwater included, to be analyzed by FT-ICR MS at the same concentrations. This option was not chosen as it would have reduced the analytical window for our focus of study: tree-DOM.

Once mixed 1:1 with methanol, samples were analyzed in negative mode electrospray ionization using a 15 Tesla FT-ICRMS (Bruker Solarix) at the University of Oldenburg, Germany. 500 broadband scans were accumulated for the mass spectra. After internal calibration, mass accuracies were within an error of <0.2 ppm. Elemental formulas were assigned to peaks with signal to noise ratios greater than five based on published rules (Koch et al., 2007; Stubbins et al., 2010; Singer et al., 2012). Peaks detected in the procedural blank (PPL extracted ultrapure water) were removed. Peak detection limits were standardized between samples by adjusting the dynamic range of each sample to that of the sample with the lowest dynamic range (dynamic range = average of the largest 20% of peaks assigned a formula divided by the signal to noise threshold intensity; standardized detection limit = average of largest 20% of peaks assigned a formula within a sample divided by the lowest dynamic range within the sample set; Spencer et al., 2014; Stubbins et al., 2014). Peaks below the standardized detection limit were removed.

These peaks were removed in order to prevent false negatives within samples with low dynamic range.

For each elemental formula, we calculated the modified Aromaticity Index (AImod) (Koch and Dittmar, 2006, 2016), which indicates the likelihood of an elemental formula representing aromatic structures, from an AImod of zero, where formulas are aliphatic, through an intermediate range, where an elemental formula could indicate aromatic or non-aromatic isomers, to AImod values above 0.5, where an elemental formula is highly likely to represent aromatic isomers (Koch and Dittmar, 2006). These AImod values were calculated as:

$$\text{AImod} = \frac{(1 + C - 0.5O - S - 0.5(N + P + H))}{(C - 0.5O - S - N - P)} \quad (1)$$

AImod values 0.5–0.67 and >0.67 were assigned as aromatic and condensed aromatic structures, respectively (Koch and Dittmar, 2006). Compound classes were further defined as highly unsaturated (AImod < 0.5, H/C < 1.5, O/C < 0.9), unsaturated aliphatics (1.5 ≤ H/C < 2, O/C < 0.9, N = 0), saturated fatty acids (H/C ≥ 2, O/C < 0.9), sugars (O/C ≥ 0.9) and peptides (1.5 ≤ H/C < 2, O/C < 0.9, N < 0). Since an individual formula could occur as multiple isomeric structures, these classifications only serve as a guide to the structures present within DOM. For instance, “peptides” have the elemental formulas of peptides, but their actual structure may differ.

Standardized peak intensities ( $z$ ) within a sample were calculated following:

$$z = \frac{x - \mu}{\sigma} \quad (2)$$

where,  $x$  is the measured peak intensity,  $\mu$  is mean peak intensity within the sample, and  $\sigma$  is the standard deviation in peak

intensity within the sample (Spencer et al., 2014). Cluster analysis of the standardized peak intensities of assigned formulas (Ward clustering in JMP®) was then performed (Spencer et al., 2014).

## RESULTS

### Dissolved Organic Matter Concentrations and Optical Properties

DOM concentrations, quantified as DOC, ranged from 1.1 to 2.4 mg-C L<sup>-1</sup> in rainwater, 40 to 95 mg-C L<sup>-1</sup> in oak stemflow, 2.2 to 28 mg-C L<sup>-1</sup> in oak throughfall, 52 to 71 mg-C L<sup>-1</sup> in epiphyte-covered cedar stemflow, 31 to 62 mg-C L<sup>-1</sup> in epiphyte-covered cedar throughfall, 25 to 30 mg-C L<sup>-1</sup> in bare cedar stemflow, and 12 to 16 mg-C L<sup>-1</sup> in bare cedar throughfall across the two storms sampled.

Absorbance spectra decayed exponentially with increasing wavelength (Figure 2). Napierian absorption coefficients for CDOM at 300 nm ranged from 0.1 to 3.2 m<sup>-1</sup> in rainwater, 101 to 526 m<sup>-1</sup> in oak stemflow, 6 to 81 m<sup>-1</sup> in oak throughfall, 321 to 378 m<sup>-1</sup> in epiphyte-covered cedar stemflow, 95 to 148 m<sup>-1</sup> in epiphyte-covered cedar throughfall, 129 to 159 m<sup>-1</sup> in bare cedar stemflow, and 36 to 67 m<sup>-1</sup> in bare cedar throughfall across the two storms sampled.

Spectral slope values for the range 275–295 nm for CDOM ranged from 0.0156 to 0.0673 nm<sup>-1</sup> in rainwater, 0.0142 to 0.0147 nm<sup>-1</sup> in oak stemflow, 0.0139 to 0.0169 nm<sup>-1</sup> in oak throughfall, 0.0145 to 0.0154 nm<sup>-1</sup> in epiphyte-covered cedar stemflow, 0.0157 to 0.0166 nm<sup>-1</sup> in epiphyte-covered cedar throughfall, 0.0145 to 0.0155 nm<sup>-1</sup> in bare cedar stemflow, and 0.0152 to 0.0165 nm<sup>-1</sup> in bare cedar throughfall across the two storms sampled.

SUVA<sub>254</sub> values ranged from 0.5 to 1.3 L mg-C<sup>-1</sup> m<sup>-1</sup> in rainwater, 1.9 to 4.2 L mg-C<sup>-1</sup> m<sup>-1</sup> in oak stemflow, 1.6 to 2.8 L mg-C<sup>-1</sup> m<sup>-1</sup> in oak throughfall, 4.0 to 5.1 L mg-C<sup>-1</sup> m<sup>-1</sup> in epiphyte-covered cedar stemflow, 2.3 to 2.8 L mg-C<sup>-1</sup> m<sup>-1</sup> in epiphyte-covered cedar throughfall, 4.0 to 4.1 L mg-C<sup>-1</sup> m<sup>-1</sup> in

bare cedar stemflow, and 2.4 to 3.3 L mg-C<sup>-1</sup> m<sup>-1</sup> in bare cedar throughfall across the two storms sampled.

The full dataset is presented in Table S1. Means and standard deviations for each data and sample type per storm are presented in Table 1 and summarized in Figure 3. Patterns in DOC concentrations and DOM optical properties were similar between storms (Figure 3). Rainwater DOM had much lower values of DOC, CDOM, and SUVA, and much steeper spectral slope values than the tree-DOM samples. In general, the stemflow samples exhibited higher DOC, CDOM, and SUVA, and shallower spectral slopes, than their respective throughfall samples (Figure 3). The one exception being DOC for the epiphyte-covered cedar during storm A, when both stemflow and throughfall DOC concentrations were similar (Figure 3A).

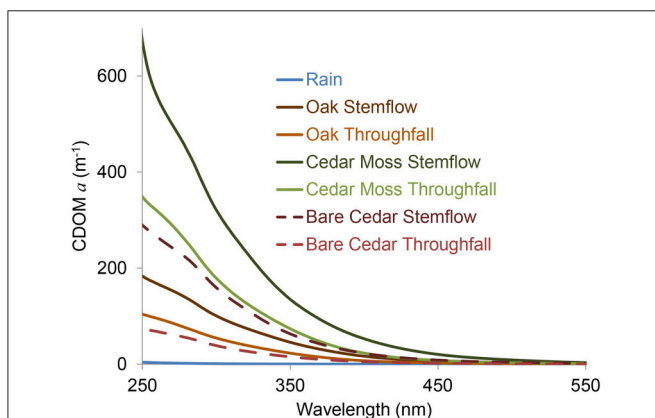


**FIGURE 2 | Exemplary colored dissolved organic matter (CDOM) Napierian absorption coefficient (a) spectra for rainwater and each of the stemflow (SF) and throughfall (TF) sample types collected.**

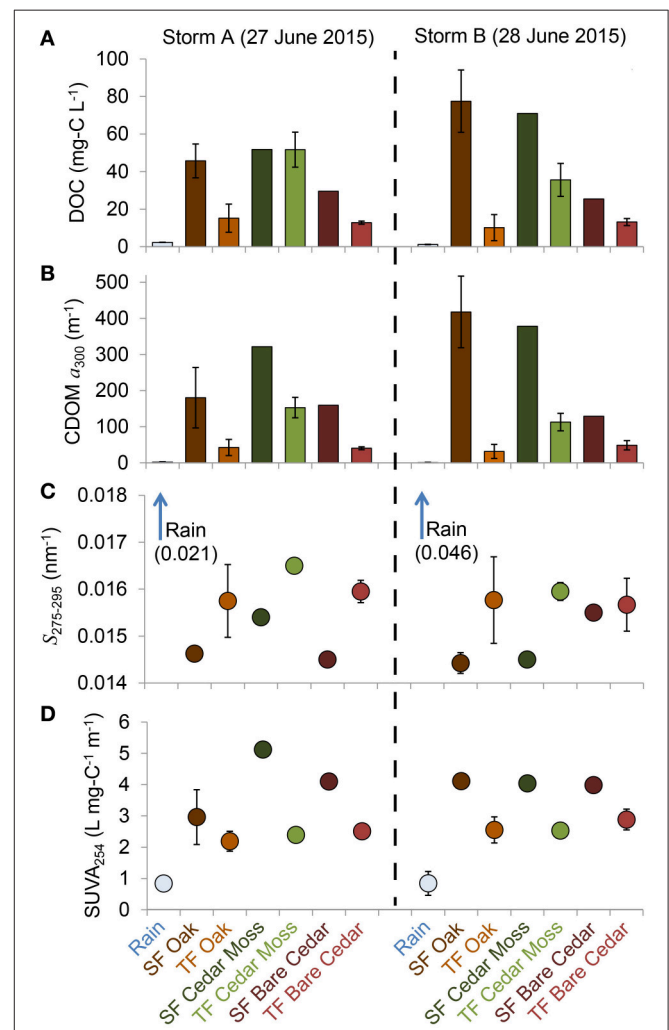


**FIGURE 3 | Mean values for (A) dissolved organic carbon (DOC) concentration, (B) colored dissolved organic matter (CDOM) Napierian absorption coefficient at 300 nm ( $a_{300}$ ), (C) spectral slope from 275 to 295 nm ( $S_{275-295}$ ), and (D) specific ultraviolet absorbance at 254 nm ( $SUVA_{254}$ ) for rainwater and each of the stemflow (SF) and throughfall (TF) sample types collected (see legend). Error bars represent 1 standard deviation and are not shown when they were narrower than the symbol.**

## Molecular Signatures of Tree-Derived Dissolved Organic Matter

Whole water samples mixed 1:1 with methanol yielded mass spectra (Figure 4) with sufficient resolution and signal to enable the assignment of 5,852 elemental formulas to tree-DOM. The raw mass spectra for oak and cedar stemflow displayed molecular signatures consistent with those of whole river water DOM run on the same instrument, under the same conditions, during the same month (Kolyma River data in Figure 4; Stubbins et al., 2017). Looking at one representative mass to charge (343 m/z; Figure 4), DOM in oak stemflow and cedar stemflow has similar molecular diversities (i.e., there are a similar number of peaks). However, the relative abundance of some peaks varies between samples, with some peaks being below detection in one sample and present in the other.

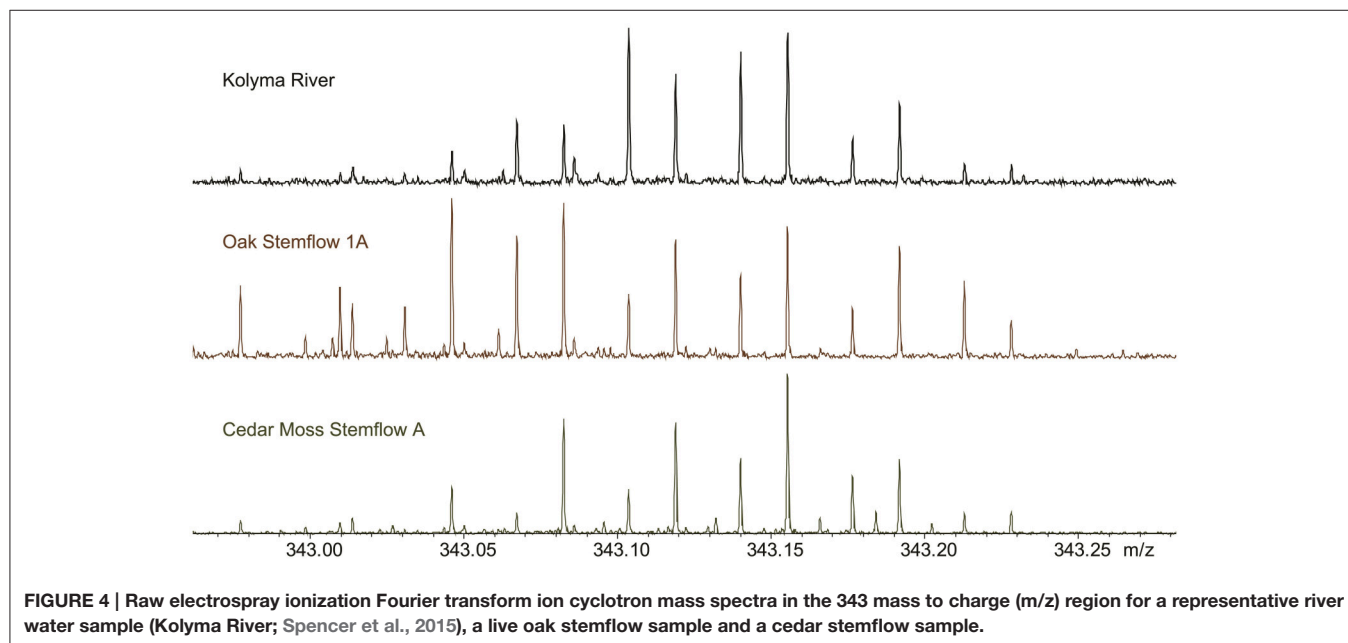
To further explore the diversity of tree-DOM and how it varied among the samples a cluster analysis of the standardized peak intensities of assigned formulas (Ward clustering in JMP<sup>®</sup>) was performed (Spencer et al., 2014). The distance graph for this cluster analysis revealed a sharp slope break at 4 clusters (Figure 5; lower panel). These four clusters were: rainwater, stemflow oak, throughfall oak, cedar, the latter including stemflow and throughfall from both the epiphyte-covered and bare cedar trees (Figure 5). Oak DOM, including both stemflow and throughfall, and cedar DOM are clearly separated (distance between clusters,  $d = 17$ ). Oak stemflow and throughfall are also separated from one another (distance between clusters,  $d = 12$ ). Although other clusters are formed, the distances between them are smaller ( $d < 6$ ). For instance, the epiphyte-covered and bare cedar trees form distinct clusters, but with a cluster distance of  $< 2$  these samples have limited molecular differences. Based upon the cluster analysis, the molecular properties of three molecularly distinct types of tree-DOM are presented: oak throughfall, oak

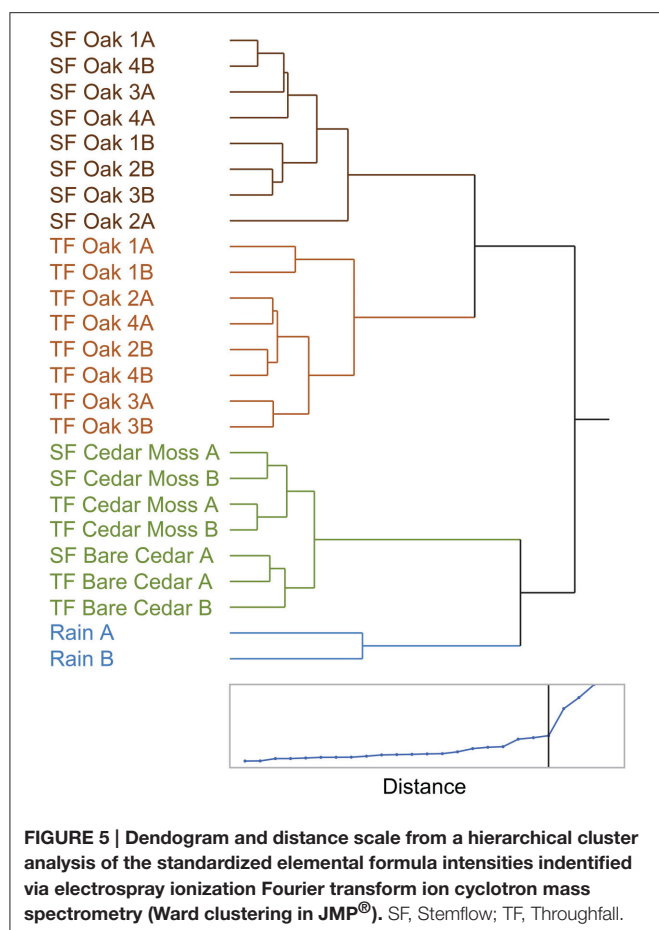
stemflow and cedar (Table 2). Data for the rainwater cluster are not presented.

The oak stemflow cluster comprised 4,765, oak throughfall 3,565, and cedar 3,643 formulas. All samples contained high proportions of CHO-only formulas (65–71%; Table 2). The oak stemflow was enriched in nitrogen compared to oak throughfall, and both were enriched in nitrogen compared to cedar DOM. Oak throughfall was enriched in sulfur and depleted in phosphorous compared to the other forms of tree-DOM, with cedar DOM being the most enriched in phosphorous.

The elemental formulas for each tree-DOM type were plotted in van Krevelen space (Figures 6A–C). Oak DOM spanned a broader range of van Krevelen space than cedar DOM. All types of tree-DOM contained high intensity elemental formulas in the region bounded by approximately H/C 1.1–1.6 and O/C 0.15 and 0.35. Oak DOM also had similarly high intensity elemental formulas in the approximate region H/C 0.5–1.0 by O/C 0.25–0.7.

All forms of tree-DOM covered a wide area of van Krevelen space and correspondingly included elemental formulas with a diverse range of possible structural properties (Table 2). All tree-DOM clusters had similar contributions from aromatic compounds (14–15%), but oak DOM was enriched in condensed aromatics (12–13%) compared to cedar DOM (10%). Highly unsaturated formulas were the most prominent molecular class in each type of tree-DOM and were enriched in cedar DOM (47%) compared to oak DOM (38–40%; Table 2). Combined aliphatics, including both unsaturated aliphatics and saturated fatty acids, constituted approximately 25% of peaks in all tree-DOM types. Sugar and peptide contributions were low across tree-DOM types, but were elevated in oak DOM compared to cedar DOM. Oak throughfall DOM had a lower average molecular mass (359 g mol<sup>-1</sup>) compared to both oak stemflow and cedar DOM (382–383 g mol<sup>-1</sup>). Average H/C and Almod





values for the clusters were similar. However, O/C decreased from oak stemflow > oak throughfall > cedar.

To reveal the quintessential molecular signatures of each tree-DOM type, the degree to which each elemental formula was enriched in a tree-DOM cluster relative to the mean for all tree-DOM types (i.e., mean intensity for a molecular formula in the whole dataset, excluding the two rain samples) was calculated as:

$$\text{Enrichment Factor} = \frac{\text{Mean Intensity in Clustered Samples}}{\text{Mean Intensity in All Tree DOM Samples}} \quad (3)$$

An elemental formula was then classified as being enriched within a tree-DOM type if it exhibited an enrichment factor >1 and also had relatively low variations in intensity across the clustered samples (standard deviation <50% of mean intensity). The standard deviation term was included in the classification in order to exclude formulas which were not routinely enriched within the samples of a cluster. The results of this classification are presented in **Table 2** and in van Krevelen diagrams (**Figures 6D–F**). Dot size in the van Krevelen diagrams represents the mean intensity of an elemental formula in the mass spectrum, while dot color represents the degree of enrichment ranging from just above 1 (yellow) to 3 or higher (dark blue). Oak stemflow was enriched in a large

number (**Table 2**) and wide variety of molecules (**Figure 6D**) compared to oak throughfall and cedar DOM (**Figures 6E,F**). However, many of the elemental formulas that were highly enriched in oak stemflow (enrichment factor >2; darker blues) were present at relatively low intensity (small size of the dots). Oak throughfall was also enriched in a wide variety of DOM types (**Figure 6E**), but had highest enrichment in the low H/C, low O/C region typical of condensed aromatics and within the region bounded by approximately H/C 1.1–1.6 and O/C 0.15 and 0.35 where the original van Krevelens (**Figures 6A–C**) revealed high abundance within all tree-DOM types. Finally, cedar DOM was enriched in elemental formulas with H/C values from approximately 1.0–1.5 and O/C 0.1–0.45 (**Figure 6F**).

Quintessential cedar DOM formulas (i.e., formulas that were consistently enriched in cedar DOM; **Table 2** right side) were enriched in CHO-only formulas (93%) compared to oak DOM (83–84%). The number of nitrogen containing quintessential formulas decreased in the order oak stemflow > oak throughfall > cedar, while sulfur containing quintessential formulas decreased in the order oak throughfall > cedar > oak stemflow, and phosphorous containing quintessential formulas decreased in the order cedar > oak stemflow > oak throughfall (**Table 2**). The average molecular mass, O/C, and AImod of quintessential oak stemflow formulas was higher than that for cedar and oak throughfall, while quintessential cedar formulas had the highest average H/C and lowest average O/C and AImod. Quintessential oak formulas were enriched in condensed aromatics (17–21%) and contained a small proportion of peptide (0.3%) and sugar (2.0–4.3%) formulas, while the quintessential cedar formulas included zero condensed aromatic, peptide or sugar formulas (**Table 2**). Quintessential oak stemflow formulas included approximately twice the percentage of aromatic formulas (23%) when compared to the other tree DOM types (12–13%). Quintessential cedar formulas were highly enriched in highly unsaturated formulas (71%), which represented approximately half of the quintessential oak stemflow formulas (53%), and about a third (30%) of quintessential oak throughfall formulas. Finally, quintessential oak throughfall formulas were enriched in unsaturated aliphatics (30%) compared to quintessential cedar (16%) and oak stemflow (5%).

Distribution plots further resolved variations in molecular mass, H/C, O/C, and AImod of the quintessential formulas that are enriched were the different tree-DOM types (**Figure 7**). Quintessential oak stemflow formulas covered a broad, relatively evenly distributed range in molecular mass, O/C, H/C and AImod, with the H/C distribution skewed toward lower values (center ~1.0; **Figure 7C**). Those formulas that were enriched in oak throughfall DOM exhibited pronounced peaks in abundance at low molecular mass (~260 g mol<sup>-1</sup>; **Figure 7A**), low O/C (~0.24; **Figure 7B**), high H/C (~1.6; **Figure 7C**), and contained three spikes in AImod (0, ~0.2 and ~0.8; **Figure 7D**). Quintessential cedar formulas also exhibited marked peaks in molecular mass (~310 g mol<sup>-1</sup>; **Figure 7A**), midranges in H/C (~1.0–1.2; **Figure 7C**) and AImod (~0.4; **Figure 7D**) and a peak in O/C that reached a maximum at ~0.36, but exhibited two smaller shoulders at 0.21 and 0.11 (**Figure 7B**).

**TABLE 2 | Molecular signatures of tree-derived dissolved organic matter (DOM) within live oak stemflow, live oak throughfall and cedar (stemflow plus throughfall).**

	Formulas within each cluster			Formulas enriched within each cluster		
	SF Oak	TF Oak	Cedar	SF Oak	TF Oak	Cedar
Total Formulas	4765	3565	3643	1887	859	322
CHO	3116 (65%)	2338 (66%)	2581 (71%)	1576 (84%)	714 (83%)	301 (93%)
With N	869 (18%)	552 (15%)	420 (12%)	254 (13%)	51 (5.9%)	0 (0%)
With S	574 (12%)	568 (16%)	403 (11%)	36 (1.9%)	92 (11%)	15 (4.7%)
With P	206 (4.3%)	107 (3%)	239 (6.6%)	21 (1.1%)	2 (0.2%)	6 (1.9%)
Condensed Aromatics	590 (12%)	471 (13%)	374 (10%)	330 (17%)	184 (21%)	0 (0%)
Aromatics	676 (14%)	549 (15%)	554 (15%)	431 (23%)	115 (13%)	39 (12%)
Highly Unsaturated	1922 (40%)	1340 (38%)	1706 (47%)	992 (53%)	258 (30%)	230 (71%)
Unsaturated Aliphatics	1134 (24%)	869 (24%)	809 (22%)	95 (5.0%)	261 (30%)	52 (16%)
Saturated Fatty Acids	43 (0.9%)	40 (1.1%)	38 (1%)	0 (0%)	1 (0.1%)	1 (0.3%)
Sugars	162 (3.4%)	135 (3.8%)	82 (2.3%)	37 (2.0%)	37 (4.3%)	0 (0%)
Peptides	244 (5.1%)	162 (4.5%)	80 (2.2%)	6 (0.3%)	3 (0.3%)	0 (0%)
Average Molecular Mass (g mol <sup>-1</sup> )	383	359	382	370	311	330
Average H/C	1.23	1.24	1.22	1.01	1.19	1.24
Average O/C	0.45	0.42	0.39	0.46	0.39	0.27
Average Almod	0.31	0.32	0.32	0.42	0.36	0.35

Percentages represent the relative contributions of each molecular class within each type of tree-DOM. Left side: values for all formulas within each type of tree-DOM. Right side: values for formulas that were enriched within each type of tree-DOM.

## DISCUSSION

### Concentrations and Optical Signatures of Tree-DOM

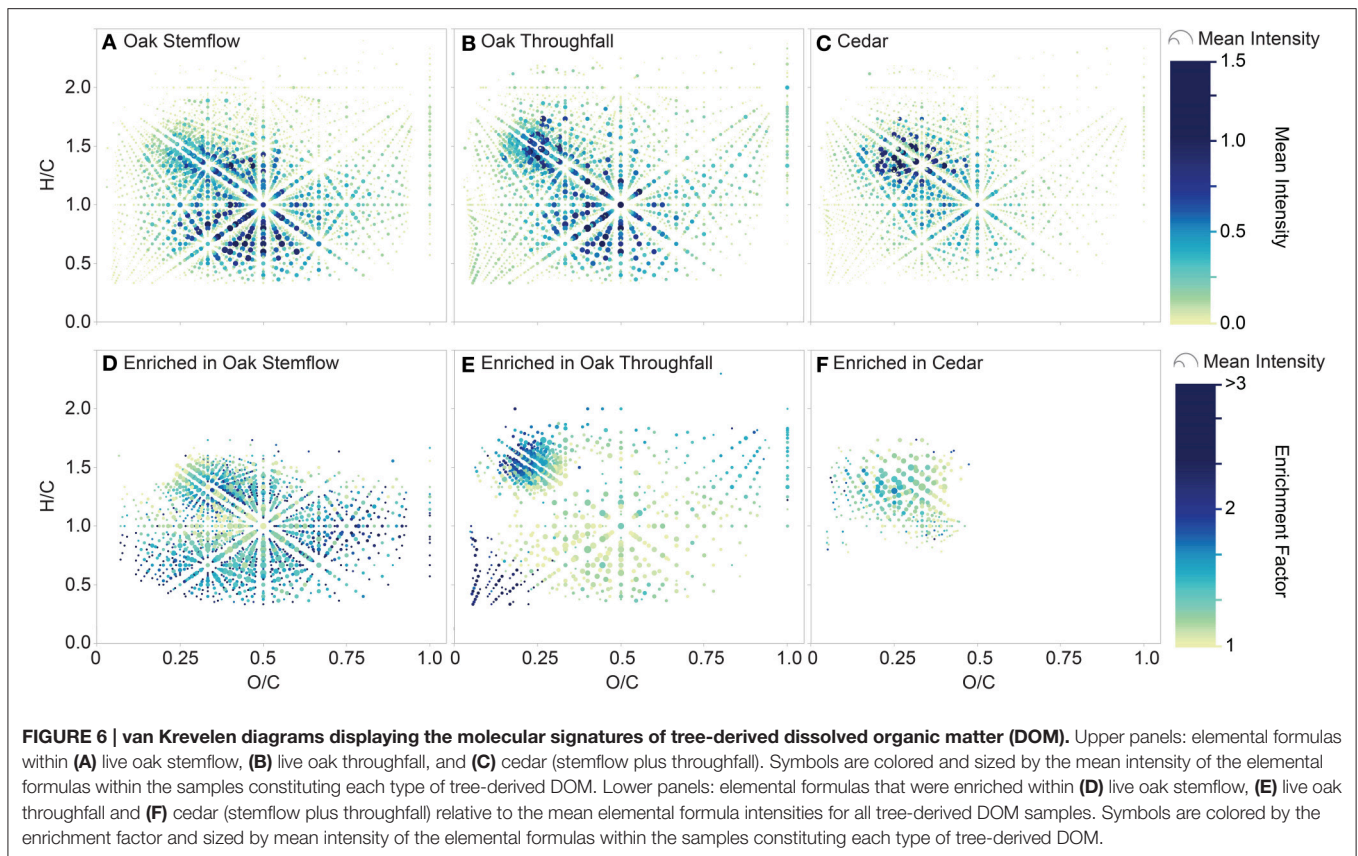
The high levels of DOC and CDOM in stemflow and throughfall relative to rainwater samples indicate that rainwater DOM was a very minor component of stemflow and throughfall DOM, with the majority of tree-DOM being entrained during interaction with the tree canopy and stem.

Mean DOC concentrations in throughfall (10–52 mg-C L<sup>-1</sup>) and stemflow (25–78 mg-C L<sup>-1</sup>) were both within the range of values reported by previous throughfall (1–100 mg-C L<sup>-1</sup>) (Michalzik et al., 2001; Neff and Asner, 2001; Le Mellec et al., 2010; Inamdar et al., 2012) and stemflow (5–200 mg-C L<sup>-1</sup>) (Moore, 2003; Tobón et al., 2004; Levia et al., 2011) studies. The observed range in tree-DOC concentrations is at the higher end or exceeds the mean DOC concentrations in major US rivers (1–12 mg-C L<sup>-1</sup>; Spencer et al., 2012), but is consistent with the high DOC values observed in black water rivers draining swamps (e.g., St. Marys = 42 mg-C L<sup>-1</sup>; Spencer et al., 2012). Given the small size of the current dataset (two storms, six trees), no estimates of DOC fluxes are made.

The optical properties of tree-DOM are broadly consistent with those for CDOM in other aquatic environments. Tree-DOM CDOM spectra exhibit an exponential increase in absorbance with decreasing wavelength (Figure 2). The range in mean spectral slope values ( $S_{275-295}$ ) for stemflow (0.0144 nm<sup>-1</sup>) and throughfall (0.0157–0.0165 nm<sup>-1</sup>) are consistent with values for US rivers (0.012–0.023 nm<sup>-1</sup>) (Spencer et al., 2012). Literature values for stemflow and throughfall spectral slope were not found for comparison. SUVA<sub>254</sub> values for stemflow (means 3.0–5.1 L

mg-C<sup>-1</sup> m<sup>-1</sup>) from our oaks and cedars compare with ranges of 2.5–4.9 L mg-C<sup>-1</sup> m<sup>-1</sup> for American beech (*Fagus grandifolia*) and 3.7–6.2 L mg-C<sup>-1</sup> m<sup>-1</sup> for yellow poplar (*Liriodendron tulipifera*) (Levia et al., 2011). These values are all at the higher end or exceeding the range in mean SUVA<sub>254</sub> values reported for US rivers (1.3–4.6 L mg-C<sup>-1</sup> m<sup>-1</sup>) (Spencer et al., 2012) and are consistent with highly colored, aromatic-rich DOM (Weishaar et al., 2003). The mean SUVA<sub>254</sub> values for throughfall (2.2–2.9 L mg-C<sup>-1</sup> m<sup>-1</sup>) compare to previous literature values for throughfall of 1.8–4.7 L mg-C<sup>-1</sup> m<sup>-1</sup> (Inamdar et al., 2012) and also indicate a significant contribution of aromatics to throughfall DOM. All tree-DOM SUVA values were higher than for rainwater CDOM and all tree-DOM spectral slopes steeper than for rainwater DOM (Figures 3C,D), indicating tree-DOM to be more aromatic than the trace amounts of DOM in rainwater. Hydrological fluxes become enriched with aromatic compounds, including lignin degradation products, as contact time with bark increases (Guggenberger et al., 1994). Therefore, the enrichment of stemflow in highly aromatic, high SUVA<sub>254</sub> DOM compared to throughfall is likely due to the high hydrological connectivity of stemflow with tree bark and other sources of tree-derived organics. The aromatics in tree-DOM are likely dominated by autochthonous, tree-produced aromatics, such as lignin, and their degradation products (Guggenberger et al., 1994) that accumulate and are then washed off the tree surface during rain events. In addition, allochthonous organics delivered to the tree via atmospheric deposition (Guggenberger and Zech, 1994) could include aromatics derived from soils, combustion sources, or distal vegetation.

The quantity, but not the optical quality of tree-DOM exported during both storms varied with epiphyte cover. DOC



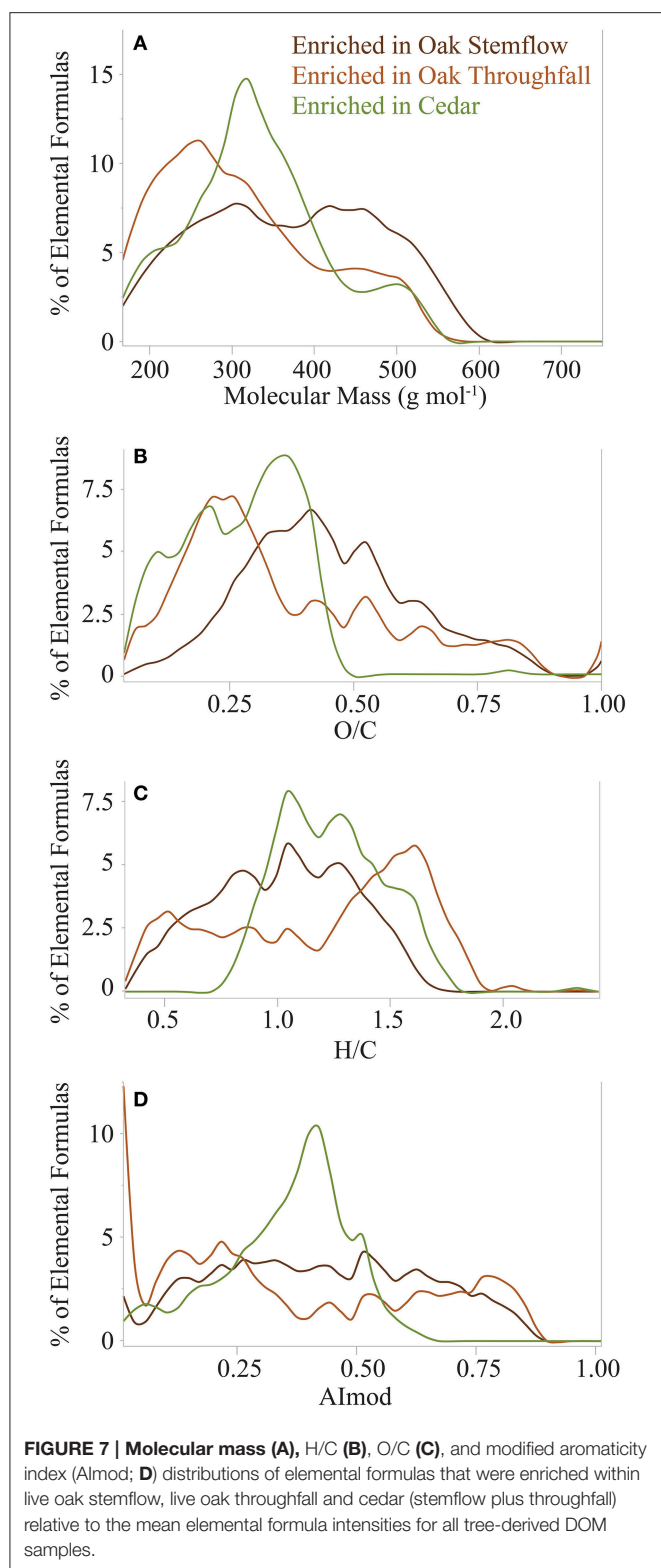
concentration and CDOM were consistently lower in both stemflow and throughfall from the bare cedar than from the epiphyte covered cedar and the four oaks, which all had mixed epiphyte cover (Table 1; Figures 1, 3). These results suggest that epiphytes were either a direct source of autochthonous, epiphyte organics or an intermediate accumulator of organics derived from the tree, fauna or atmospheric deposition. Research into the fluxes and quality of epiphyte DOM release is scarce. With respect to the dominant epiphytes encountered in our study, no data is available for resurrection ferns; while Spanish moss collected from nearby sites in coastal Georgia leached DOM with significantly lower SUVA<sub>254</sub> values (Van Stan et al., 2015) than for the current tree-DOM samples (Table 1). The Spanish moss samples leached in Van Stan et al. (2015) were cleaned of all canopy soil and any decaying or damaged moss. As such, these leachates contained organics derived directly from Spanish moss rather than from the more diverse canopy ecosystem and potential organic sources that the presence of Spanish moss in a tree cultivates. For the limited data collected in our study (two storms, six trees, one of which has no epiphyte cover), the presence of epiphytes increased DOC concentrations, but did not reduce the SUVA<sub>254</sub> values as would be expected if the additional DOC leached directly from healthy Spanish moss. Therefore, the DOM enrichment within stemflow and throughfall exported by epiphyte covered trees is likely due to the increase in hydrological contact time and flow path (Levia and Frost, 2003), the accumulation of organic matter from bark, litter

and fauna facilitated by the presence of epiphytes in the canopy ecosystem (Hietz et al., 2002; Woods et al., 2012), and potentially, the increase in canopy surface area for atmospheric deposition (Rodrigo et al., 1999; Woods et al., 2012).

## Molecular Signatures of Tree-DOM

The molecular signatures of whole water tree-DOM as revealed by negative mode electrospray ionization FT-ICR MS (Figure 2) share many features of whole water and extracted DOM from other aquatic environments (Mopper et al., 2007; Singer et al., 2012; Chen et al., 2014; Dittmar and Stubbins, 2014; Cawley et al., 2016). Shared features include a high diversity of elemental formulas distributed broadly in van Krevelen space (Figures 6A–C) and spanning a range of molecular classes (Table 2). The average molecular mass of tree-DOM (359–382 g mol<sup>-1</sup>; Table 2) was greater than for Kolyma River whole water DOM run on the same mass spectrometer (336 g mol<sup>-1</sup>) (Spencer et al., 2015), but lower than for Congo River whole water DOM run on a different mass spectrometer (424 g mol<sup>-1</sup>) (Stubbins et al., 2010). Tree-DOM was also H-poor (H/C 1.22–1.24) and O-rich (O/C 0.39–0.45) compared to Kolyma River DOM (H/C 1.27; O/C 0.39) (Spencer et al., 2015). Average H/C and O/C were not reported for Congo River DOM (Stubbins et al., 2010). Other reports of elemental formulas for non-extracted river water DOM are scarce.

As for other whole water FT-ICR mass spectra for terrigenous DOM from freshwater environments (Stubbins et al., 2010,



2012a; Spencer et al., 2015), tree-DOM was dominated by CHO-only formulas and was rich in highly unsaturated molecules (Table 2). As they have a high degree of isomeric freedom, any single highly unsaturated elemental formula may represent a

diverse array of structures of correspondingly diverse potential biogeochemical sources and functions (Stubbins et al., 2010). For instance, the possible isomers of any highly unsaturated formula include aromatic ring containing lignin degradation products derived from vascular land plants (Stubbins et al., 2010) and carboxylic-rich alicyclic molecules (Hertkorn et al., 2006) of indeterminate, potentially microbial origin. Due the high SUVA<sub>254</sub> values of tree-DOM and particularly stemflow DOM, it is likely that a significant proportion of the unsaturated formulas within tree-DOM represent vascular plant derived molecules that contain aromatic rings.

The modified aromaticity index classifies formulas as either aromatic or condensed aromatic (Koch and Dittmar, 2006, 2016). Tree-DOM was enriched in aromatic formulas (14–15%; Table 2) compared to Congo River whole water analyzed on a different FT-ICR mass spectrometer (9%) (Stubbins et al., 2010), but similar in aromatic content to Kolyma River whole water analyzed on the FT-ICR mass spectrometer used in the current study (13%) (Spencer et al., 2015) consistent with the view that river DOM is derived predominantly from the degradation products of vascular plants (Ertel et al., 1984) and the enrichment of similar compounds within tree-DOM.

Tree-DOM was also enriched in condensed aromatics (10–12%; Table 2) compared to both Congo (1%) (Stubbins et al., 2010) and Kolyma River (6%) (Spencer et al., 2015) samples. Condensed aromatics are known to form during the incomplete combustion of organics (Goldberg, 1985) and when observed in DOM are usually termed dissolved black carbon and ascribed a thermogenic source (Kim et al., 2004; Hockaday et al., 2006; Ziolkowski and Druffel, 2010). The ubiquity of dissolved black carbon in river waters (Dittmar et al., 2012; Jaffé et al., 2013; Stubbins et al., 2015; Wagner et al., 2015) is explained as resulting from the ubiquity of refractory, apparently thermogenic black carbon in soils (Forbes et al., 2006; Guggenberger et al., 2008; Schmidt et al., 2011). Other sources of black carbon to natural waters and landscapes include direct input from local combustion sources and atmospheric deposition from distant combustion sources. Atmospheric deposition has been posited as a source of organics to remote regions of the earth (Stubbins et al., 2012a; Spencer et al., 2014) and organics transported from global and regional sources of combustion (e.g., automobile, industrial, domestic, agricultural, wildfire, and biomass burning), as well as produced locally on the Skidaway Institute of Oceanography campus, could all produce black carbon for deposition to the trees sampled.

Aliphatic formulas (sum of unsaturated aliphatics and saturated fatty acids) were slightly enriched in tree-DOM (23–25%; Table 2) relative to Congo (19%) (Stubbins et al., 2010) and Kolyma River (22%) (Spencer et al., 2015) DOM. Tree-DOM was also enriched in sugar (2.3–3.8%) and peptide (2.2–5.1%) formulas compared to Kolyma River DOM (0.6% sugar; 2.2% peptide) (Spencer et al., 2015). Sugar and peptide formulas were not reported for the Congo River (Stubbins et al., 2010). All of these compound classes likely derive directly from foliar leachates, foliar washoff, and their breakdown products (Guggenberger and Zech, 1994; Michalzik et al., 2001; Kalbitz et al., 2007). However, similar molecular formulas

are also observed in atmospheric aerosols (Wozniak et al., 2008).

## Quintessential Signatures of Oak Stemflow, Oak Throughfall and Cedar DOM

Tree-DOM molecular signatures were significantly different from rainwater DOM and clustered in three groups: oak stemflow, oak throughfall and cedar, the latter including stemflow and throughfall samples from both the epiphyte covered and bare cedars (Figure 5). Distinct differences between the molecular signatures of each class of tree-DOM were evident in van Krevelen plots (Figures 6A–C). In order to determine the elemental formulas that distinguished these three classes of tree-DOM from one another, the quintessential formulas associated with each type of tree-DOM were classified as those formulas that are consistently enriched across the samples within a cluster (Equation 3). Plotting the resultant data in van Krevelen space revealed that the above data treatment accentuated differences in the molecular signatures of oak stemflow, oak throughfall, and cedar DOM (Figures 6D–F). As noted in the results, dot size in the van Krevelen diagrams (Figures 6D–F) represents the mean intensity of an elemental formula in the mass spectrum, while dot color represents the degree of enrichment ranging from just above 1 (yellow) to 3 or higher (dark blue).

Quintessential oak stemflow formulas (Figure 6D) occupied much of the van Krevelen space typically populated by riverine DOM (e.g., Spencer et al., 2015 in which data for a Kolyma River whole water sample run on the same mass spectrometer is displayed). The van Krevelen is densely populated, as is also typical of riverine DOM samples. The enrichment of stemflow DOM in this diverse population of formulas indicates that the organics within oak stemflow are of more diverse origin or have undergone more extensive processing than the organics within oak throughfall and cedar DOM. The canopy structure and coarse bark of live oaks makes them excellent habitats for colonization by epiphytes, such as the Spanish moss and resurrection ferns observed on our sampled trees (Figure 1d), the accumulation of organic debris, and utilization by fauna. The development of these canopy microhabitats, replete with observable canopy soils within the trees on SkIO campus, may have led to the development of a rich molecular mix of organics for export. While of diverse stoichiometric composition, the quintessential oak stemflow elemental formulas were of higher average molecular mass and AImod (Table 2; Figure 7A), and enriched in aromatics, compared to quintessential oak throughfall and cedar formulas, suggestive of the greater interaction of stemflow with the oak bark, debris and canopy soils.

Quintessential oak throughfall formulas (Figure 6E) were not as evenly distributed in van Krevelen space as the quintessential formulas of oak stemflow suggesting formulas enriched in throughfall derive from more distinct sources and have undergone less processing. Compared to the quintessential formulas associated with oak stemflow and cedar, quintessential oak throughfall formulas were of low average molecular weight

(311 g mol<sup>-1</sup>) and were enriched in unsaturated aliphatics (30%) and sugars (4.3%; Table 2), suggesting significant inputs from the direct leaching or washing of foliar surfaces (Guggenberger and Zech, 1994; Michalzik et al., 2001; Kalbitz et al., 2007). Oak throughfall also contained elevated levels of condensed aromatics (21%; Table 2; Figure 7B) compared to the other tree-DOM classes, suggesting potential wash off of deposited combustion products from leaf surfaces.

By comparison to oak DOM, cedar DOM was enriched in CHO-only and highly unsaturated formulas (Table 2) of limited molecular diversity (Figure 6F; Figure 7C), suggesting cedar DOM is enriched in minimally processed non-descript tree-DOM.

## CONCLUSIONS

The relatively high SUVA<sub>254</sub> values and abundance of aliphatics and aromatic formulas within tree-DOM are consistent with autochthonous (i.e., tree-derived) organics. However, the presence of condensed aromatics within tree-DOM also suggests that some of the DOM exported from trees derives from the atmospheric deposition of allochthonous organics. As electrospray ionization efficiency varies with analyte chemistry, the current dataset cannot be used to robustly quantify the contribution of condensed aromatics or other forms of deposited organics to tree-DOM export. Future work should therefore seek to quantify the contribution of condensed aromatics and other allochthonous forms of DOM to tree-DOM to assess how much of the tree-DOM flux is derived from autochthonous vs. allochthonous sources.

As the crowning headwaters of the terrestrial hydrological cycle, tree canopies are the point of first contact between precipitation and terrestrial ecosystems. The quality of tree-DOM as detailed by absorbance and FT-ICR MS is similar to the terrigenous DOM described in inland waters, but sufficiently distinct that optical and chemical signatures may be of use in tracking tree-DOM into receiving ecosystems including forest floor soils and inland waters. Further study is required to develop an understanding of the fate and ecological functions of tree-DOM within receiving ecosystems. Such knowledge will be essential in assessing how ongoing changes to forest cover distributions will impact both soil and aquatic ecosystems.

## AUTHOR CONTRIBUTIONS

AS wrote the paper with input from other authors. AS and JV designed the study. LS collected the samples, analyzed samples and worked up the DOC and CDOM data sets. AS and TD analyzed the samples by FT-ICR MS and worked up the FT-ICR MS data.

## SUPPLEMENTARY MATERIAL

The Supplementary Material for this article can be found online at: <http://journal.frontiersin.org/article/10.3389/feart.2017.00022/full#supplementary-material>

## REFERENCES

- Aitkenhead-Peterson, J., McDowell, W., Neff, J., Stuart, E., and Robert, L. (2003). "Sources, production, and regulation of allochthonous dissolved organic matter inputs to surface waters" in *Aquatic Ecosystems Interactivity of Dissolved Organic Matter*, eds S. E. G. Findlay and R. L. Sinsabaugh (New York, NY: Academic Press), 26–70. doi: 10.1016/b978-012256371-3/50003-2
- Algeo, T. J., Scheckler, S. E., and Maynard, J. B. (2001). "Effects of the middle to late devonian spread of vascular land plants on weathering regimes, Marine Biotas, and Global Climate," in *Plants Invade the Land: Evolutionary and Environmental Approaches*, eds P. G. Gensel and D. Edwards (New York, NY: Columbia University Press), 213–236.
- Cawley, K. M., Murray, A. E., Doran, P. T., Kenig, F., Stubbins, A., Chen, H., et al. (2016). Characterization of dissolved organic material in the interstitial brine of Lake Vida, Antarctica. *Geochim. Cosmochim. Acta* 183, 63–78. doi: 10.1016/j.gca.2016.03.023
- Chen, H., Stubbins, A., Perdue, E. M., Green, N. W., Helms, J. R., Mopper, K., et al. (2014). Ultrahigh resolution mass spectrometric differentiation of dissolved organic matter isolated by coupled reverse osmosis-electrodialysis from various major oceanic water masses. *Mar. Chem.* 164, 48–59. doi: 10.1016/j.marchem.2014.06.002
- Crutzen, P. J. (2002). Geology of mankind. *Nature* 415, 23–23. doi: 10.1038/415023a
- Dittmar, T., De Rezende, C. E., Manecki, M., Niggemann, J., Coelho Ovalle, A. R., Stubbins, A., et al. (2012). Continuous flux of dissolved black carbon from a vanished tropical forest biome. *Nat. Geosci.* 5, 618–622. doi: 10.1038/ngeo1541
- Dittmar, T., and Stubbins, A. (2014). "Dissolved Organic Matter in Aquatic Systems," in *Treatise on Geochemistry, 2nd Edn.*, ed K. K. Turekian (Oxford: Elsevier), 125–156.
- Ertel, J. R., Hedges, J. I., and Perdue, E. M. (1984). Lignin signature of aquatic humic substances. *Science* 223, 485–487. doi: 10.1126/science.223.4635.485
- FAO (2016). "State of the World's Forests 2016," in *Forests and Agriculture: Land-Use Challenges and Opportunities* (Rome).
- Forbes, M. S., Raison, R. J., and Skjemstad, J. O. (2006). Formation, transformation and transport of black carbon (charcoal) in terrestrial and aquatic ecosystems. *Sci. Total Environ.* 370, 190–206. doi: 10.1016/j.scitotenv.2006.06.007
- Gensel, P. G. (2001). "Introduction," in *Plants Invade the Land: Evolutionary and Environmental Approaches*, eds P. G. Gensel and D. Edwards (New York, NY: Columbia University Press), 1–2.
- Georgia Office of the State Climatologist (2012). *Office of the State Climatologist*. Available online at: <https://epd.georgia.gov/office-state-climatologist> (Accessed September 13, 2013).
- Goldberg, E. (1985). *Black Carbon in the Environment*. New York, NY: Wiley.
- Greb, S. F., DiMichele, W. A., and Gastaldo, R. A. (2006). "Evolution and importance of wetlands in earth history," in *Wetlands Through Time*, eds W. A. DiMichele and S. Greb (Boulder, CO: Geological Society of America), 1–40.
- Guggenberger, G., Rodionov, A., Shubitova, O., Grabe, M., Kasansky, O. A., Fuchs, H., et al. (2008). Storage and mobility of black carbon in permafrost soils of the forest tundra ecotone in Northern Siberia. *Glob. Chang. Biol.* 14, 1367–1381. doi: 10.1111/j.1365-2486.2008.01568.x
- Guggenberger, G., and Zech, W. (1994). Composition and dynamics of dissolved carbohydrates and lignin-degradation products in two coniferous forests, NE Bavaria, Germany. *Soil Biol. Biochem.* 26, 19–27. doi: 10.1016/0038-0717(94)90191-0
- Guggenberger, G., Zech, W., and Schulten, H.-R. (1994). Formation and mobilization pathways of dissolved organic matter: evidence from chemical structural studies of organic matter fractions in acid forest floor solutions. *Org. Geochem.* 21, 51–66. doi: 10.1016/0146-6380(94)90087-6
- Hansen, M. C., Potapov, P. V., Moore, R., Hancher, M., Turubanova, S., Tyukavina, A., et al. (2013). High-resolution global maps of 21st-century forest cover change. *Science* 342, 850–853. doi: 10.1126/science.1244693
- Hansen, M. C., Stehman, S. V., and Potapov, P. V. (2010). Quantification of global gross forest cover loss. *Proc. Natl. Acad. Sci. U.S.A.* 107, 8650–8655. doi: 10.1073/pnas.0912668107
- Helms, J. R., Stubbins, A., Ritchie, J. D., Minor, E. C., Kieber, D. J., and Mopper, K. (2008). Absorption spectral slopes and slope ratios as indicators of molecular weight, source, and photobleaching of chromophoric dissolved organic matter. *Limnol. Oceanogr.* 53, 955–969. doi: 10.4319/lo.2008.53.3.0955
- Hertkorn, N., Benner, R., Frommberger, M., Schmitt-Kopplin, P., Witt, M., Kaiser, K., et al. (2006). Characterization of a major refractory component of marine dissolved organic matter. *Geochim. Cosmochim. Acta* 70, 2990–3010. doi: 10.1016/j.gca.2006.03.021
- Hietz, P., Wanek, W., Wania, R., and Nadkarni, N. M. (2002). Nitrogen-15 natural abundance in a montane cloud forest canopy as an indicator of nitrogen cycling and epiphyte nutrition. *Oecologia* 131, 350–355. doi: 10.1007/s00442-002-0896-6
- Hockaday, W. C., Grannas, A. M., Kim, S., and Hatcher, P. G. (2006). Direct molecular evidence for the degradation and mobility of black carbon in soils from ultrahigh-resolution mass spectral analysis of dissolved organic matter from a fire-impacted forest soil. *Org. Geochem.* 37, 501–510. doi: 10.1016/j.orggeochem.2005.11.003
- Hu, C., Muller-Karger, F. E., and Zepp, R. G. (2002). Absorbance, absorption coefficient, and apparent quantum yield: a comment on common ambiguity in the use of these optical concepts. *Limnol. Oceanogr.* 47, 1261–1267. doi: 10.4319/lo.2002.47.4.1261
- Inamdar, S., Finger, N., Singh, S., Mitchell, M., Levia, D., Bais, H., et al. (2012). Dissolved organic matter (DOM) concentration and quality in a forested mid-Atlantic watershed, USA. *Biogeochemistry* 108, 55–76. doi: 10.1007/s10533-011-9572-4
- Jaffé, R., Ding, Y., Niggemann, J., Vähätalo, A. V., Stubbins, A., Spencer, R. G. M., et al. (2013). Global charcoal mobilization from soils via dissolution and riverine transport to the oceans. *Science* 340, 345–347. doi: 10.1126/science.1231476
- Jardine, P., McCarthy, J., and Weber, N. (1989). Mechanisms of dissolved organic carbon adsorption on soil. *Soil Sci. Soc. Am. J.* 53, 1378–1385. doi: 10.2136/sssaj1989.03615995005300050013x
- Kaiser, K., and Zech, W. (1998). Soil dissolved organic matter sorption as influenced by organic and sesquioxide coatings and sorbed sulfate. *Soil Sci. Soc. Am. J.* 62, 129–136. doi: 10.2136/sssaj1998.03615995006200010017x
- Kaiser, K., and Zech, W. (2000). Sorption of dissolved organic nitrogen by acid subsoil horizons and individual mineral phases. *Eur. J. Soil Sci.* 51, 403–411. doi: 10.1046/j.1365-2389.2000.00320.x
- Kalbitz, K., Meyer, A., Yang, R., and Gerstberger, P. (2007). Response of dissolved organic matter in the forest floor to long-term manipulation of litter and throughfall inputs. *Biogeochemistry* 86, 301–318. doi: 10.1007/s10533-007-9161-8
- Kim, S., Kaplan, L. A., Benner, R., and Hatcher, P. G. (2004). Hydrogen-deficient molecules in natural riverine water samples - Evidence for the existence of black carbon in DOM. *Mar. Chem.* 92, 225–234. doi: 10.1016/j.marchem.2004.06.042
- Koch, B. P., and Dittmar, T. (2006). From mass to structure: an aromaticity index for high-resolution mass data of natural organic matter. *Rapid Commun. Mass Spectrometry* 20, 926–932. doi: 10.1002/rcm.2386
- Koch, B. P., and Dittmar, T. (2016). From mass to structure: an aromaticity index for high-resolution mass data of natural organic matter. *Rapid Commun. Mass Spectrometry* 30, 250–250. doi: 10.1002/rcm.7433
- Koch, B. P., Dittmar, T., Witt, M., and Kattner, G. (2007). Fundamentals of molecular formula assignment to ultrahigh resolution mass data of natural organic matter. *Anal. Chem.* 79, 1758–1763. doi: 10.1021/ac061949s
- Kolka, R. K., Nater, E., Grigal, D., and Verry, E. (1999). Atmospheric inputs of mercury and organic carbon into a forested upland/bog watershed. *Water Air Soil Pollut.* 113, 273–294. doi: 10.1023/A:1005020326683
- Le Mellec, A., Meessenburg, H., and Michalzik, B. (2010). The importance of canopy-derived dissolved and particulate organic matter (DOM and POM) – comparing throughfall solution from broadleaved and coniferous forests. *Ann. For. Sci.* 67:411. doi: 10.1051/forest/2009130
- Levia, D. F., and Frost, E. E. (2003). A review and evaluation of stemflow literature in the hydrologic and biogeochemical cycles of forested and agricultural ecosystems. *J. Hydrol.* 274, 1–29. doi: 10.1016/S0022-1694(02)00399-2
- Levia, D. F., Van Stan, I., John, T., Inamdar, S. P., Jarvis, M. T., Mitchell, M. J., et al. (2011). Stemflow and dissolved organic carbon cycling: temporal variability in concentration, flux, and UV-Vis spectral metrics in a temperate broadleaved deciduous forest in the eastern United States. *Can. J. Forest Res.* 42, 207–216. doi: 10.1139/x11-173
- McClain, M. E., Boyer, E. W., Dent, C. L., Gergel, S. E., Grimm, N. B., Groffman, P. M., et al. (2003). Biogeochemical hot spots and hot moments

- at the interface of terrestrial and aquatic ecosystems. *Ecosystems* 6, 301–312. doi: 10.1007/s10021-003-0161-9
- Michalzik, B., Kalbitz, K., Park, J.-H., Solinger, S., and Matzner, E. (2001). Fluxes and concentrations of dissolved organic carbon and nitrogen—a synthesis for temperate forests. *Biogeochemistry* 52, 173–205. doi: 10.1023/A:1006441620810
- Moore, T. (2003). Dissolved organic carbon in a northern boreal landscape. *Glob. Biogeochem. Cycles* 17, 1109. doi: 10.1029/2003GB002050
- Mopper, K., Kieber, D. J., and Stubbins, A. (2015). “Marine photochemistry: processes and impacts,” in *Biogeochemistry of Marine Dissolved Organic Matter, 2nd Edn.*, eds D. A. Hansell and C. A. Carlson (New York, NY: Elsevier), 389–450.
- Mopper, K., Stubbins, A., Ritchie, J. D., Bialk, H. M., and Hatcher, P. G. (2007). Advanced instrumental approaches for characterization of marine dissolved organic matter: extraction techniques, mass spectrometry, and nuclear magnetic resonance spectroscopy. *Chem. Rev.* 107, 419–442. doi: 10.1021/cr050359b
- Neff, J. C., and Asner, G. P. (2001). Dissolved organic carbon in terrestrial ecosystems: synthesis and a model. *Ecosystems* 4, 29–48. doi: 10.1007/s100210000058
- Raymond, P. A., and Saiers, J. E. (2010). Event controlled DOC export from forested watersheds. *Biogeochemistry* 100, 197–209. doi: 10.1007/s10533-010-9416-7
- Raymond, P. A., Saiers, J. E., and Sobczak, W. V. (2016). Hydrological and biogeochemical controls on watershed dissolved organic matter transport: pulse-shunt concept. *Ecology* 97, 5–16. doi: 10.1890/14-1684.1
- Rodrigo, A., Avila, A., and Gomez-Bolea, A. (1999). Trace metal contents in *Parmelia caperata* (L.) Ach. Compared to bulk deposition, throughfall and leaf-wash fluxes in two holm oak forests in Montseny (NE Spain). *Atmos. Environ.* 33, 359–367. doi: 10.1016/S1352-2310(98)00167-8
- Schmidt, M. W. I., Torn, M. S., Abiven, S., Dittmar, T., Guggenberger, G., Janssens, I. A., et al. (2011). Persistence of soil organic matter as an ecosystem property. *Nature* 478, 49–56. doi: 10.1029/2008GB003327
- Singer, G. A., Fasching, C., Wilhelm, L., Niggemann, J., Steier, P., Dittmar, T., et al. (2012). Biogeochemically diverse organic matter in Alpine glaciers and its downstream fate. *Nat. Geosci.* 5, 710–714. doi: 10.1038/ngeo1581
- Spencer, R. G. M., Butler, K. D., and Aiken, G. R. (2012). Dissolved organic carbon and chromophoric dissolved organic matter properties of rivers in the USA. *J. Geophys. Res. Biogeosciences* 117, G03001. doi: 10.1029/2011jg001928
- Spencer, R. G. M., Guo, W., Raymond, P. A., Dittmar, T., Hood, E., Fellman, J., et al. (2014). Source and biolability of ancient dissolved organic matter in glacier and lake ecosystems on the Tibetan Plateau. *Geochim. Cosmochim. Acta* 142, 64–74. doi: 10.1016/j.gca.2014.08.006
- Spencer, R. G. M., Mann, P. J., Dittmar, T., Eglinton, T. I., McIntyre, C., Holmes, R. M., et al. (2015). Detecting the signature of permafrost thaw in Arctic rivers. *Geophys. Res. Lett.* 42, 2830–2835. doi: 10.1002/2015GL063498
- Stein, W. E., Mannolini, F., Hernick, L. V., Landing, E., and Berry, C. M. (2007). Giant cladoxypsid trees resolve the enigma of the Earth's earliest forest stumps at Gilboa. *Nature* 446, 904–907. doi: 10.1038/nature05705
- Stubbins, A., and Dittmar, T. (2012). Low volume quantification of dissolved organic carbon and dissolved nitrogen. *Limnol. Oceanogr.* 10, 347–352. doi: 10.4319/lom.2012.10.347
- Stubbins, A., and Dittmar, T. (2015). Illuminating the deep: molecular signatures of photochemical alteration of dissolved organic matter from North Atlantic Deep Water. *Mar. Chem.* 177, 318–324. doi: 10.1016/j.marchem.2015.06.020
- Stubbins, A., Hood, E., Raymond, P. A., Aiken, G. R., Sleighter, R. L., Hernes, P. J., et al. (2012a). Anthropogenic aerosols as a source of ancient dissolved organic matter in glaciers. *Nat. Geosci.* 5, 198–201. doi: 10.1038/ngeo1403
- Stubbins, A., Lapierre, J. F., Berggren, M., Prairie, Y. T., Dittmar, T., and del Giorgio, P. A. (2014). What's in an EEM? Molecular Signatures Associated with Dissolved Organic Fluorescence in Boreal Canada. *Environ. Sci. Technol.* 48, 10598–10606. doi: 10.1021/es502086e
- Stubbins, A., Law, C. S., Uher, G., and Upstill-Goddard, R. C. (2011). Carbon monoxide apparent quantum yields and photoproduction in the Tyne estuary. *Biogeosciences* 8, 703–713. doi: 10.1029/2009GL041158
- Stubbins, A., Mann, P. J., Powers, L., Bittar, T. B., Dittmar, T., McIntyre, C. P., et al. (2017). Low photolability of yedoma permafrost dissolved organic carbon. *J. Geophys. Res.* 122, 200–211. doi: 10.1002/2016JG003688
- Stubbins, A., Niggemann, J., and Dittmar, T. (2012b). Photo-lability of deep ocean dissolved black carbon. *Biogeosciences* 9, 1661–1670. doi: 10.1029/2008GL036169
- Stubbins, A., Spencer, R. G. M., Chen, H., Hatcher, P. G., Mopper, K., Hernes, P. J., et al. (2010). Illuminated darkness: molecular signatures of Congo River dissolved organic matter and its photochemical alteration as revealed by ultrahigh precision mass spectrometry. *Limnol. Oceanogr.* 55, 1467–1477. doi: 10.1890/0012-09658
- Stubbins, A., Spencer, R., Mann, P. J., Holmes, R. M., McClelland, J., Niggemann, J., et al. (2015). Utilizing colored dissolved organic matter to derive dissolved black carbon export by Arctic Rivers. *Front. Earth Sci.* 3:63. doi: 10.3389/feart.2015.00063
- Tobón, C., Sevink, J., and Verstraten, J. M. (2004). Solute fluxes in throughfall and stemflow in four forest ecosystems in northwest Amazonia. *Biogeochemistry* 70, 1–25. doi: 10.1023/B:BIOG.0000049334.10381.f8
- Van Stan, J. T., Stubbins, A., Bittar, T., Reichard, J. S., Wright, K. A., and Jenkins, R. B. (2015). *Tillandsia usneoides* (L.) L. (Spanish moss) water storage and leachate characteristics from two maritime oak forest settings. *Ecology* 8, 988–1004. doi: 10.1002/eco.1549
- Vidon, P., Allan, C., Burns, D., Duval, T. P., Gurwick, N., Inamdar, S., et al. (2010). Hot spots and hot moments in riparian zones: potential for improved water quality management. *J. Am. Water Resour. Assoc.* 46, 278–298. doi: 10.1111/j.1752-1688.2010.00420.x
- Wagner, S., Cawley, K. M., Rosario-Ortiz, F. L., and Jaffé, R. (2015). In-stream sources and links between particulate and dissolved black carbon following a wildfire. *Biogeochemistry* 124, 145–161. doi: 10.1007/s10533-015-0088-1
- Weishaar, J. L., Aiken, G. R., Bergamaschi, B. A., Fram, M. S., Fujii, R., and Mopper, K. (2003). Evaluation of specific ultraviolet absorbance as an indicator of the chemical composition and reactivity of dissolved organic carbon. *Environ. Sci. Technol.* 37, 4702–4708. doi: 10.1021/es030360x
- Wiley, J. D., Kieber, R. J., Eymann, M. S., and Avery, G. B. (2000). Rainwater dissolved organic carbon: concentrations and global flux. *Glob. Biogeochem. Cycles* 14, 139–148. doi: 10.1029/1999gb900036
- Woods, C. L., Hunt, S. L., Morris, D. M., and Gordon, A. M. (2012). Epiphytes influence the transformation of nitrogen in coniferous forest canopies. *Boreal Environ. Res.* 17, 411–425.
- Wozniak, A., Bauer, J., Sleighter, R., Dickhut, R., and Hatcher, P. (2008). Technical Note: molecular characterization of aerosol-derived water soluble organic carbon using ultrahigh resolution electrospray ionization Fourier transform ion cyclotron resonance mass spectrometry. *Atmos. Chem. Phys.* 8, 5099–5111. doi: 10.5194/acp-8-5099-2008
- Ziolkowski, L. A., and Druffel, E. R. M. (2010). Aged black carbon identified in marine dissolved organic carbon. *Geophys. Res. Lett.* 37, L16601. doi: 10.1016/j.dr.2009.05.008

**Conflict of Interest Statement:** The authors declare that the research was conducted in the absence of any commercial or financial relationships that could be construed as a potential conflict of interest.

Copyright © 2017 Stubbins, Silva, Dittmar and Van Stan. This is an open-access article distributed under the terms of the Creative Commons Attribution License (CC BY). The use, distribution or reproduction in other forums is permitted, provided the original author(s) or licensor are credited and that the original publication in this journal is cited, in accordance with accepted academic practice. No use, distribution or reproduction is permitted which does not comply with these terms.